ISIJ International, Vol. 53 (2013), No. 3, pp. 419–426

Effect of Circulating Elements on the Dynamic Reduction Swelling Behaviour of Olivine and Acid Iron Ore Pellets under Simulated Blast Furnace Shaft Conditions

Mikko ILJANA,[1)]* Olli MATTILA,[2)] Tuomas ALATARVAS,[1)] Jari KURIKKALA,[3)] Timo PAANANEN[2)] and Timo FABRITIUS[1)]

1) University of Oulu, Laboratory of Process Metallurgy, PO Box 4300, University of Oulu, FI-90014 Finland.
2) Ruukki Metals Oy, Rautaruukintie 155, Raahe, FI-92100 Finland.
3) Boliden Harjavalta Oy, Teollisuuskatu 1, Harjavalta, FI-29200 Finland.

(*Received on October 24, 2012; accepted on December 10, 2012*)

Sulphur and alkalis in the blast furnace gas have been associated affecting the reduction swelling behaviour of iron ore pellets. A tube furnace was used in this study to examine the dynamic reduction swelling behaviour of olivine and acid pellets in $CO–CO_2–N_2$ atmosphere with sulphur and potassium in gaseous phases up to 1 100°C simulating the conditions in the blast furnace shaft.

No abnormal swelling was detected in sulphur or potassium containing $CO–CO_2–N_2$ atmospheres during dynamic reduction. Instead, sulphur in the reducing atmosphere was associated with pellet contraction and FeO–FeS melt formation which became more dominant with increasing sulphur partial pressures. In the extreme case, having a maximum of 1.0 vol-% S_2 gas in the reducing atmosphere, the reduction reaction of wüstite to metallic iron was hindered. The formation of FeO–FeS liquid phase extends the cohesive zone towards the blast furnace top and lower temperatures and decreases the gas permeability. Furthermore, large amounts of potassium in the reducing atmosphere (max. 0.03 vol-%) led to swelling and cracking in the olivine pellets still remaining in the range of normal swelling.

KEY WORDS: olivine pellet; acid pellet; sulphur; potassium; reduction; swelling; cracking; non-isothermal condition; blast furnace.

1. Introduction

The most common circulating elements in the blast furnace are sulphur, alkalis (Na, K), zinc and silicon. Especially sulphur and alkalis have led to a debate, because in some cases they have caused operational difficulties in the blast furnaces. In the literature, sulphur and alkalis in the blast furnace gas have been associated affecting the reduction swelling behaviour of iron ore pellets.

Alkalis enter the blast furnace in raw materials in the form of complex silicates such as alkali-alumino-silicates.[1)] Potassium usually accumulates to higher levels than sodium in the blast furnaces[2,3)] and the main reactions relating to potassium circulation are described here. Potassium silicate, K_2SiO_3, is the most stable potassium compound below 1 000°C in the prevailing blast furnace conditions. At temperatures exceeding 1 000–1 100°C, it begins to decompose according to Eqs. (1) and (2), producing K and KCN vapours.[4)]

$$K_2SiO_3(s,l) + CO(g) = 2K(g) + CO_2(g) + SiO_2(s) \quad \text{..... (1)}$$

$$K_2SiO_3(s,l) + 5CO(g) + N_2(g) = 2KCN(s,l,g) + 3CO_2(g) + SiO_2(g) \quad \text{..... (2)}$$

The alkali and alkali cyanide vapours formed in the hot zone of the blast furnace rise with the gases towards lower temperatures where the condensation of the alkalis becomes possible. The alkalis can accumulate inside the blast furnace in the form of cyanides, carbonates and intercalation compounds in coke (C_6K, C_8K, $C_{24}K$, *etc.*).[1)] The condensation of the alkalis to silicates occurs at temperatures below 1 000°C (Eqs. (1) and (2) backwards), or alternatively to alkali carbonates, which are less stable compounds than alkali silicates, according to Eqs. (3) and (4).[4)]

$$2K(g) + 2CO_2(g) = K_2CO_3(s) + CO(g) \quad \text{..... (3)}$$

$$2KCN(g) + 4CO_2(g) = K_2CO_3(s) + 5CO(g) + N_2(g) \quad \text{..... (4)}$$

The condensed alkali compounds descend with charge materials towards the hot reducing zone, where the carbonates and other less stable compounds react first, followed by the silicates at higher temperatures, liberating the alkalis again into the gas phase and circulation.[4)]

Sulphur enters the blast furnace with metallurgical coke and hydrocarbon fuels but also with iron bearing materials.

* Corresponding author: E-mail: mikko.iljana@oulu.fi
DOI: http://dx.doi.org/10.2355/isijinternational.53.419

Sulphur is in the form of sulphides or sulphates in raw materials. Most of the sulphur from coke and hydrocarbon fuels burn in the oxidizing zone in front of the tuyeres generating SO_2 gas. SO_2 reacts with carbon immediately after passing the oxidizing zone and forms carbon-based compounds, such as COS and CS. In addition to chemical reactions, sulphur in charge materials is released in gasification. Sulphur in different gaseous phases ascends to the upper parts in the blast furnace and absorbs in the descending charge materials and reduced iron. In the blast furnace process, sulphur can exist dissolved in the hot metal, as sulphides (*e.g.* CaS, FeS) in the slag or as various components (*e.g.* S_2, SO_2, CS_2, COS, H_2S) in the gas phase. In the upper parts of the blast furnace, sulphur mainly exists in the form of COS and H_2S and in the hot reducing zone as CS_2.[5–7)]

In the literature, sulphur has been associated with pellet volume change, both swelling and contraction.[2,8–13)] It has been reported that even small amounts of gaseous sulphur accelerate the reduction of wüstite.[14)] Hooey *et al.*[12)] pinpoint that a small amount of sulphur addition to the reducing gas in the swelling test can cause catastrophic swelling and thus totally change the reduction swelling behaviour of the pellets verified in some laboratory experiments with S_2 gas. Furthermore, Hooey *et al.*[12)] highlight that sulphur compounds, as well as other potentially significant trace components in the blast furnaces, are not included in any standard tests, thus limiting the reliability of the experimental results.

Hayashi and Iguchi[2,10)] have studied the effect of gaseous sulphur and the addition of K_2CO_3 to pelletizing mixture on the swelling during reduction of hematite pellets. According to their study, both gaseous sulphur and addition of potassium carbonate promote pellet swelling, the effect of gaseous sulphur on the amount of swelling being more dominant. The volume increase was 500% at the most due to whisker formation when sulphur present in the reducing atmosphere. Later, Hayashi[13)] reported the formation of Fe–O–S and Fe–S liquid in H_2 gas atmosphere with small amounts of H_2S gas at 1 000°C and 1 300°C. These liquid phases were concentrated on the pellet periphery. Already at lower temperatures of 800°C solid FeS was verified on the pellet periphery area in the cross-sections of the polished samples after reduction. Also, Lee and Rhee[15)] noticed the formation of a compact iron sulphide (FeS) layer on the pellet surface during reduction of iron oxide pellets under the hydrogen sulphide (1–3 vol-% H_2S) containing atmosphere. Partial pressures of sulphur below the formation limit of FeS have been associated with the formation of porous-reduced iron and iron whiskers leading to the overall swelling of the reducing iron burden structure.[10,15)]

The effect of potassium on the reduction swelling behaviour has been investigated only in a few studies. Bahgat *et al.*[16)] found that swelling and the reduction rate of wüstite compacts both decreased with increasing K_2O content. The effect of sodium on the swelling of hematite during reduction has been studied by Lu.[17)] In that study, hematite specimens with various amounts of Na_2CO_3 were heat-treated under reducing conditions and the addition of sodium carbonate seemed to promote cracking and swelling during reduction.

In this paper, the effect of circulating elements (S, alkalis) in the blast furnace on the reduction swelling behaviour of olivine and acid iron ore pellets have been discussed based on a comprehensive series of laboratory experiments carried out under simulated blast furnace shaft conditions. Potassium was selected as a typical alkali because it usually accumulates to higher contents than sodium in the blast furnaces.[2,3)]

2. Materials and Methods

Commercial olivine pellets and acid pellets were used in the investigations performed. Olivine pellets were manually separated into three grades of low, medium and high magnetic, representing the size of the magnetite nucleus, using a custom made device. The olivine pellet grades were named “LoMag”, “MeMag” and “HiMag” respectively and the acid pellet “RefPellet”. The divalent iron (FeO) content of the olivine pellet fractions was 0.1 wt-%, 0.2 wt-% and 2.9 wt-%, respectively. Detailed descriptions of the sample preparation and the experimental procedure are given in the earlier paper[18)] as well as the chemical analysis of the pellets. The equations for determining the degree of reduction and reduction swelling index (RSI) are also presented there.

Additionally, the cracking index was used to describe the overall cracking tendency of pellets obtained from the experiments. Samples of each experiment were classified visually according to type images of the cracked structure. Type 0 indicates “none” cracking whereas index value 3 represents the “extremely cracked” structure. Example images are shown in **Fig. 1**.

In addition to the operational description of the Blast Furnace gas phase Simulator (BFS) presented in the earlier paper,[18)] adjusting the partial pressure of sulphur and potassium is introduced here. The partial pressure of potassium was adjusted by controlling the temperature of the reactor vessel beneath the main furnace leading to controlled reaction rates (with carrier gas) between sieved graphite chippings and potassium carbonate. The reaction produces mainly monoatomic potassium and carbon monoxide gases

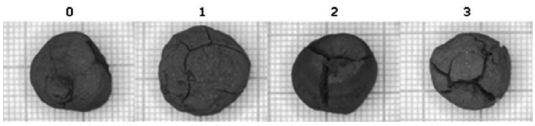

Fig. 1. Classification of the cracking structure.

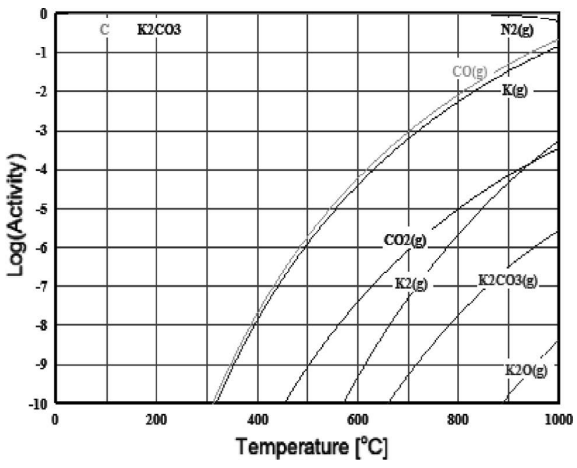

Fig. 2. Equilibrium composition for the system in the potassium generator.

(see Eq. (5)) as can be seen in the equilibrium composition graph of the system consisting of C, K_2CO_3 and their possible gas components (see **Fig. 2**). The equilibrium composition has been calculated with HSC Chemistry 7.00 thermodynamic calculation software.

$$K_2CO_3(s) + 2C(s) = 2K(g) + 3CO(g) \quad \text{..... (5)}$$

The partial pressure of sulphur was controlled by the mass flow controller of the sulphur dioxide gas to the reactor vessel containing sieved graphite chippings (1.1–3.0 mm) heated to a constant temperature of 800°C. In the vessel, the sulphur dioxide gas reacts with graphite chippings to produce S_2 and CO_2 gases according to Eq. (6). Furthermore, some COS, CO and CS_2 are generated and some SO_2 remains unreacted. Later in the furnace tube, same sulphur-containing compounds are likely to form than in a real blast furnace except for hydrogen sulphides. According to the study by Blomster *et al.*,[19] the yield of diatomic sulphur gas is at the highest level in temperatures near 800°C when reducing sulphur dioxide to elemental sulphur by solid carbon. The sulphur generator acts also as a pre-heating system of feed gas and the bottom part of the furnace. The amount of CO generated in the potassium generator and the amount of CO_2 in the sulphur generator have been taken into account in the computer system controlling the reducing atmosphere so that the addition of sulphur or potassium do not affect the ability of gases to reduce iron oxides in the furnace tube.

$$2SO_2(g) + 2C(s) = S_2(g) + 2CO_2(g) \quad \text{..... (6)}$$

As potassium and sulphur are present in the gas phase, the condensation must be taken into account. **Figure 3** presents the vapour pressure of monoatomic potassium and diatmomic sulphur as a function of temperature. The graph has been drawn based on the data in HSC Chemistry 7.00. It can be seen that the condensation of potassium occurs at temperatures below 260°C when the partial pressure of potassium is 10^{-4} atm (corresponds 0.01 vol-% K in the reducing atmosphere) but the temperature in the furnace is higher, except for the very first minutes in the experiments. In the reduction swelling tests, the feed of SO_2 through the sulphur generator was started at 500°C, thus at roughly a 50°C higher temperature than the boiling point of diatomic sulphur (see Fig. 3). Hence, the condensation of sulphur is not possible to occur inside the furnace tube.

In each reduction swelling experiment, two olivine pellets of each grade were selected together with two acid pellets. Each swelling experiment followed the same operation line in the Fe–O–CO–CO_2 phase diagram presented in the earlier paper.[18] The operation line simulates the temperature and the CO/CO_2 ratio in the blast furnace shaft and is consistent with the general understanding of how CO–CO_2 gas composition changes in the blast furnace shaft.[20–23] The basic gas composition and temperature conditions in the reduction swelling tests are shown in **Fig. 4**. The total gas volume flow rate was 10 l/min in each reduction swelling experiment.

The basic atmosphere profile was modified with three levels of sulphur partial pressures and two levels of potassium partial pressures. Sulphur partial pressure was elevated towards higher temperatures being a maximum of 0.01 vol-% in the "Low-S", 0.10 vol-% in the "Medium-S" and 1.0 vol-% in the "High-S" experiment. Investigations of the quenched Hirohata No. 1 blast furnace showed shaft areas where the sulphur content in the gas phase exceeded 0.1 vol-%. The "High-S" experiment is an estimate of the extreme case when using a high amount of sulphur-containing hydrocarbon fuel. The maximum content of sulphur has been calculated according to mass balances of a real blast furnace and the effect of the sulphur circulation is taken into account multiplying the sulphur content in the gas phase by 4–5 times from the charged amount. The effect of potassium on

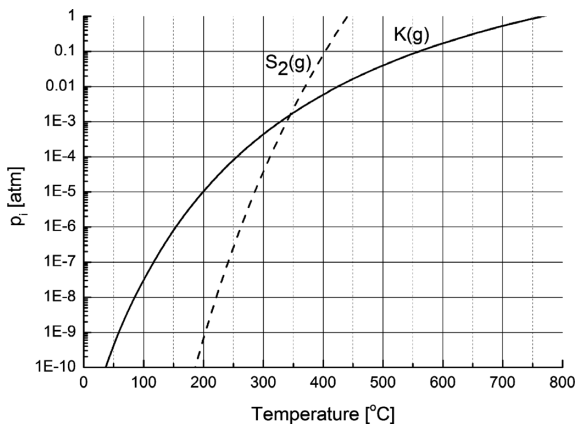

Fig. 3. Vapour pressure of K and S_2 as a function of temperature.

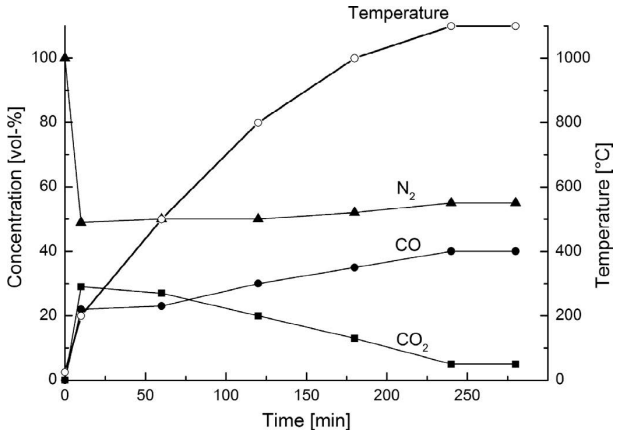

Fig. 4. Basic gas atmosphere and temperature profiles as a function of time in the reduction swelling tests.

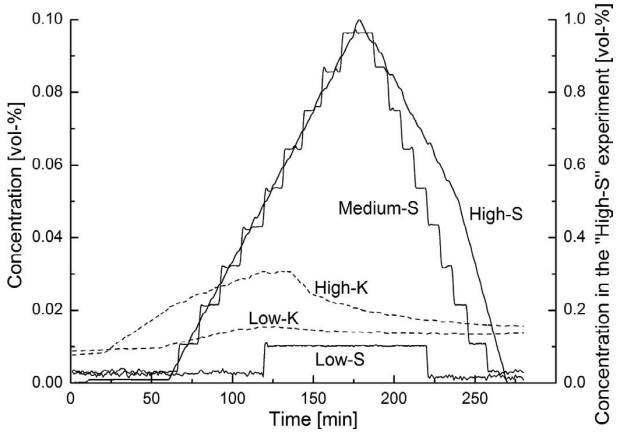

Fig. 5. Concentration of minor gas components in sulphur and potassium containing reduction swelling experiments. The scale of the "High-S" experiment is marked in the right axis of the graph.

pellet swelling was tested with two experiments, the first one containing a maximum of 0.015 vol-% potassium and the latter one a maximum of 0.03 vol-% during the experiment. The potassium concentration used in the reduction swelling experiments was determined based on the measurements in a Japanese blast furnace.[3] According to these measurements, the vapour pressure of potassium is 3.7×10^{-4} atm at 900–1 000°C and 8.2×10^{-4} atm in the temperature range from 1 000°C to 1 200°C. The concentration of sulphur and potassium as a function of the experimental time is depicted in **Fig. 5**.

3. Results

The reduction swelling indices and the degrees of reduction are calculated as averages for different pellet grades and the whole eight-pellet sample in each experiment. No numerical values for the reduction swelling behaviour of single pellets are reported here.

Pellet images after swelling experiments are shown in **Fig. 6**. In the "High-S" experiment both olivine and acid pellets melted at elevated temperatures. It can be seen that large amounts of potassium in the reducing atmosphere enhances crack formation in the olivine pellets. Cracking behaviour of olivine pellets tends to be somewhat an individual feature of a pellet even if pellets are separated into three grades based on differences in magnetic characteristics. However, acid pellets are markedly less vulnerable to crack during reduction.

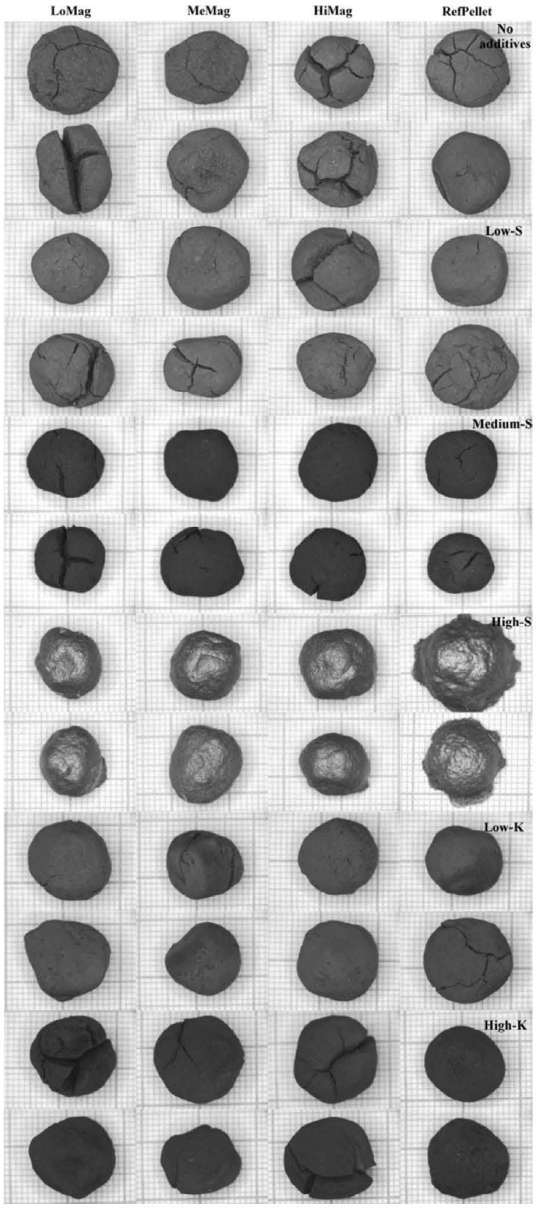

Fig. 6. Pellet cracking in the reduction swelling experiments. The upper images in each experiment represent sample no. 1 and the lower ones no. 2.

Figure 7 shows the average reduction swelling indices of the whole eight-pellet sample as a function of the average degree of reduction under certain reducing conditions. The figure indicates that sulphur in reducing atmosphere leads to pellet volume decrease, but large amounts of potassium to volume increase being 10.5% at the most.

The sum of cracking indices in the dynamic reduction swelling experiments is shown in **Fig. 8** except for the "High-S" experiment. The cracking index of the pellet grades in each experiment is a sum of the cracking indices of two pellets of the same grade. The figure depicts clearly that olivine pellets encompass more and larger cracks than acid pellets. Furthermore, it shows that the high-magnetite fraction is the most vulnerable to cracking during reduction in the olivine pellets.

The average reduction swelling indices and average degrees of reduction for different pellet grades in sulphur-containing reduction swelling experiments are presented in **Fig. 9**. The volume of acid pellets in the "Medium-S" experiment decreased markedly during reduction, but not such a

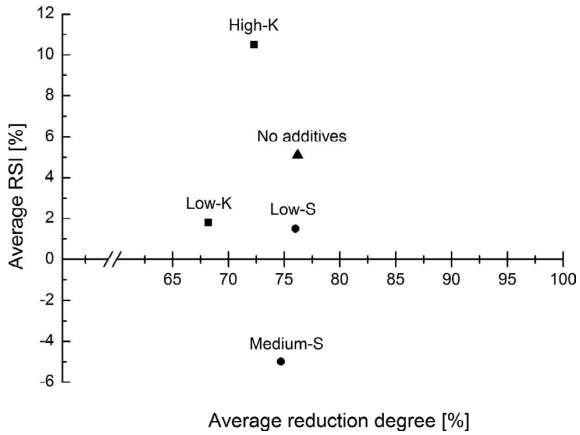

Fig. 7. Average reduction swelling indices as a function of the average degree of reduction under certain reducing conditions.

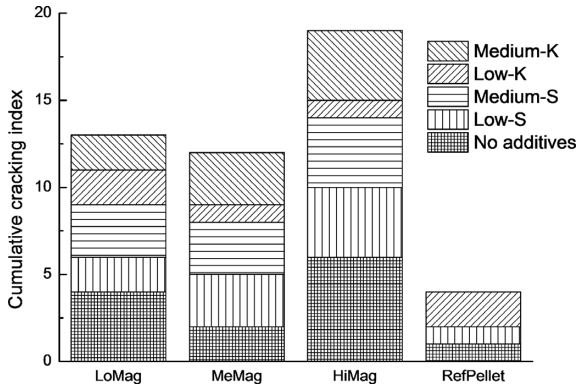

Fig. 8. Sum of cracking indices in dynamic reduction without and with additives.

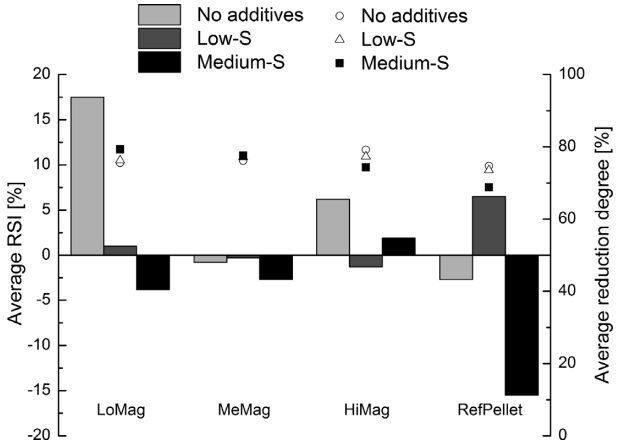

Fig. 9. Average reduction swelling indices (columns) and average degrees of reduction (dots) for different pellet grades in dynamic reduction in CO–CO_2–N_2 atmosphere with gaseous sulphur.

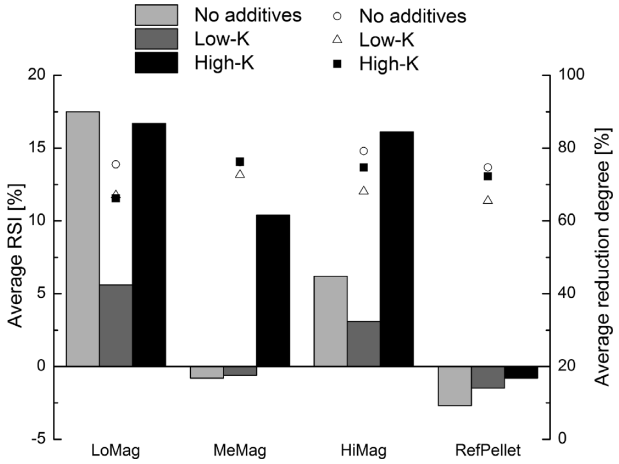

Fig. 10. Average reduction swelling indices (columns) and average degrees of reduction (dots) for different pellet grades in dynamic reduction in CO–CO_2–N_2 atmosphere with gaseous potassium.

visible effect in the olivine pellets can be seen mainly being a consequence of the crack formation during reduction. Because of the melt formation the degree of reduction of the pellets was not possible to be determined in the "High-S" experiment.

The average reduction swelling indices and the average degrees of reduction for different pellet grades in dynamic reduction in CO–CO_2–N_2 atmosphere with gaseous potassium are presented in **Fig. 10**. Swelling behaviour in the "Low-K" experiment showed even lower levels of overall swelling when compared to the reference experiment without additional gases. But large amounts of gaseous potassium in reducing atmosphere were noticed to lead to an overall volume increase in the pellets. Acid pellets contracted in each reduction swelling experiment with gaseous potassium, but the volume change decreased with increased amount of potassium in the reducing atmosphere.

4. Discussion

No catastrophic swelling was observed under reducing conditions with gaseous sulphur either in the olivine pellets or in the acid pellets unlike in some pellet grades in the

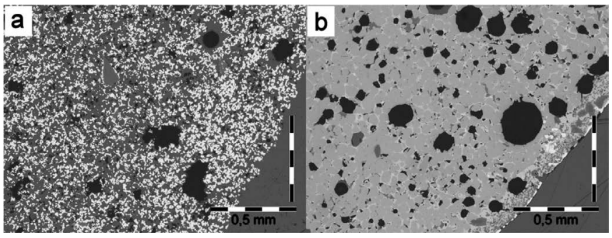

Fig. 11. LOM images from the periphery of a low-magnetite olivine pellet after (a) the "Medium-S" experiment and (b) the "High-S" experiment.

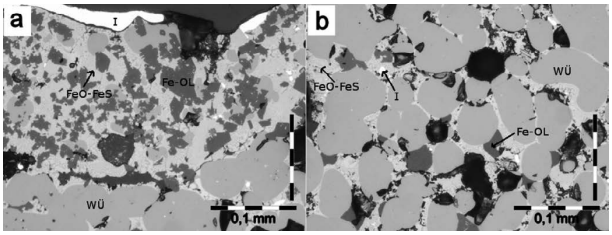

Fig. 12. LOM images from the periphery (a) and the core (b) of a medium-magnetite olivine pellet in the "High-S" experiment. "I" stands for metallic iron, "Fe-OL" for Fe-rich olivine and "WÜ" for wüstite.

study by Hooey *et al.*[12] Olivine pellets were shown to encompass more and larger cracks than acid pellets under dynamic conditions in CO–CO_2–N_2 atmosphere with or without sulphur or potassium. This is due to the dualistic structure of a magnetite nucleus and a hematite shell in the olivine pellets, and a higher gangue content and different slag chemistry making cohesive slag bonds in the acid pellets. Additionally, the olivine pellets with a large magnetite nucleus were shown to crack most significantly and olivine pellets to have a higher deviation in RSI values than acid pellets. The swelling mechanism of olivine and acid pellets is more precisely discussed in the earlier paper by authors.[18]

In the "High-S" experiment – representing the extreme case of the sulphur concentration in the blast furnace atmosphere – the pellets began to melt and partially penetrated through the sample basket leading also to the partial melting of the basket and the furnace tube and to totally different internal structure of pellets compared to the experiments with lower sulphur partial pressures. Light optical microscope (LOM, Olympus BX51) images from the periphery of a low-magnetite olivine pellet after (a) the "Medium-S" experiment and (b) the "High-S" experiment are shown in **Fig. 11**. In the "Medium-S" experiment remarkable amounts of coarse-structured metallic iron has been formed but in the "High-S" experiment round-shaped wüstite is the dominating phase and metallic iron grains were only detected on the outermost pellet periphery.

Figure 12 presents comparative LOM images captured from the periphery and the core of a medium-magnetite olivine pellet under the highest sulphur partial pressure conditions ("High-S" experiment). Phases have been verified by a field emission scanning electron microscope (FESEM, Zeiss Ultra Plus) with an EDS detector. The samples were coated with carbon before EDS analyses to ensure electrical conductivity. In the periphery image, the pellet rim reposes up. Around the pellet a dense metallic shell has been formed due to sintering of iron grains. Additionally, a high partial

pressure of sulphur in the gas has led to the formation of FeO–FeS phase especially on the pellet periphery and the volume of pellets decreased due to melt formation.

Figure 13 depicts an EDS mapping of elements from the periphery of a low-magnetite olivine pellet reduced in the "High-S" experiment. The lighter the colour of a certain element, the higher the concentration is. It can be noticed that sulphur has been concentrated near the pellet periphery but has also diffused into the inner structure of the pellet between phase boundaries. More precisely, FeS melt was verified to exist in the grain boundaries of wüstite (FeO) as can be seen in **Fig. 14**. The chemical composition of the point 1 was analysed with FESEM-EDS to be 74.0 wt-% Fe and 18.6 wt-% O corresponding to the mineralogical formula of $Fe_{1.14}O$ and 62.8 wt-% Fe and 35.5 wt-% S for the analysis point 2 corresponding to the mineralogical formula of $Fe_{1.02}S$. Judging from the microscopic study, gaseous sulphur is able to diffuse into the pellet core among grain boundaries. Lee and Rhee[15] and Hayashi[13] have also noticed the formation of a similar compact iron sulphide layer on the pellet surface under H_2S containing conditions.

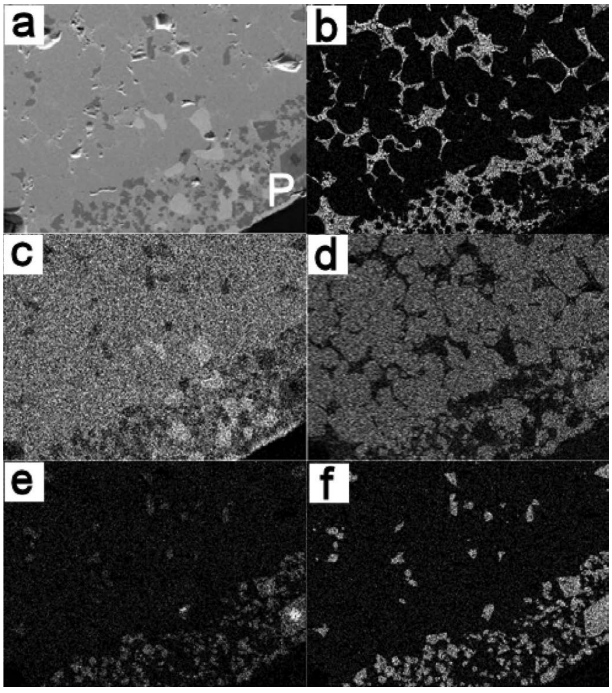

Fig. 13. FESEM-EDS mapping of elements in a low-magnetite olivine pellet in the "High-S" experiment. Figure (a) is the original backscattered electron image and the EDS mapping of elements is presented in (b) S, (c) Fe, (d) O, (e) Mg and (f) Si. The pellet periphery is marked with P in the image (a).

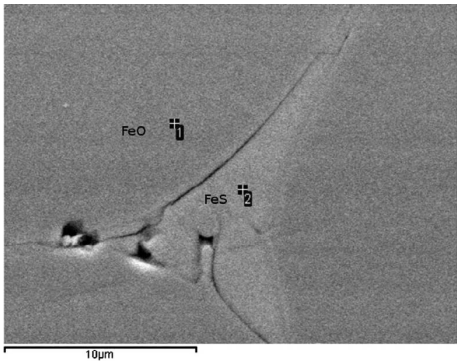

Fig. 14. Iron sulphide (FeS) liquid phase on the grain boundaries of wüstite (FeO).

The phase diagram of iron-saturated melts in the system FeO–FeS by Oelson[24] and Schürmann and von Hertwig[24] shows that the lowest liquidus temperature in the high sulphur area of the system is as low as 910°C. This leads to the partial melting of the pellets and decreases the cracking of the pellets. **Figure 15** depicts the Fe–O–S phase stability diagram at 1 000°C as the partial pressure of sulphur was at the highest level in the reduction swelling experiments. The phase stability diagram has been drawn with HSC Chemistry 7.00 thermodynamic calculation software. The operation point in each sulphur-containing experiment is marked with a dot in the figure. The leftmost dot depicts the circumstances in the "Low-S" experiment, the rightmost dot in the "High-S" experiment and the dot between them is the "Medium-S" experiment. The figure depicts that even sulphur partial pressure as low as 10^{-7} corresponding to 0.00001 vol-% S_2 in the reducing gas makes the unstoichiometric iron sulphide ($Fe_{0.877}S$) be the most stable phase at 1 000°C. This prerequisite of sulphur partial pressure is fulfilled in each of the three sulphur-containing experiments. The Fe–O–S phase stability diagram declares why no metallic iron was formed in the "High-S" experiment and FeS–FeO dominated the whole pellet cross-section.

As a conclusion of sulphur-containing experiments, it can be stated that moderate amounts of gaseous sulphur can protect iron ore pellets against swelling in a blast furnace and prevent the charge from blocking, but excessive amounts of sulphur lead to the formation of FeO–FeS liquid phase which melts at relatively low temperatures and thus impedes the reducing gases to penetrate to the pellet core and slows down the reduction reactions. This Fe–O–S liquid phase has a major influence on the softening behaviour of the blast furnace burden like Orrebo[6] states. Furthermore, the cohesive zone expands to the upper parts in the blast furnace shaft towards lower temperatures and weakens the permeability of the burden.

In the literature, the effect of potassium on the swelling of iron ore pellets has not yet been explained unambiguously. The reduction swelling results attained in this study indicate that large amounts of potassium in the reducing atmosphere

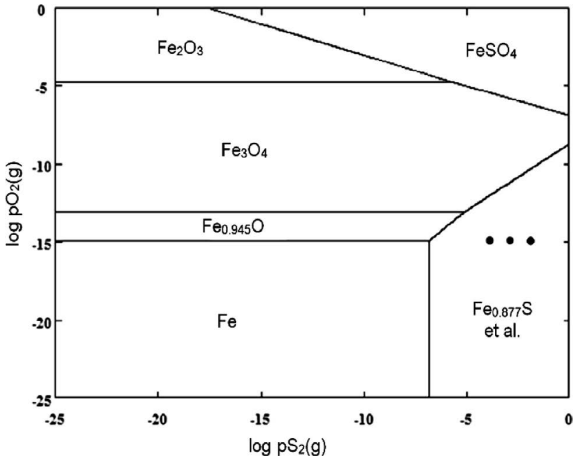

Fig. 15. Fe–O–S phase stability diagram at 1 000°C and the operation point in each sulphur-containing experiment marked with a dot.

promote pellet swelling, nevertheless including within the range of normal swelling (up to 20% in volume[16]). The observation is opposite to the study by Bahgat *et al.*,[16] in which swelling clearly decreased with increasing the amount of added K_2O to wüstite compacts during isothermal reduction. However, it must be taken into account that potassium was added as K_2O there, not being in the gaseous form. Further in the study by Bahgat *et al.*,[16] the reduction rate decreased with increasing the amount of added K_2O, the influence of potassium being similar to the present study.

The effect of alkali metal oxides (K_2O and Na_2O) on the reduction swelling behaviour of hematite was investigated by Nishikawa *et al.*[25] They reported abnormal swelling when synthetic Fe_2O_3 crystals were reacted with K_2O and Na_2O. According to their study, the addition of Na or K has three effects on the swelling behaviour of Fe_2O_3 crystals. First of all, in the initial stage of the reduction fine cracks appear in the crystals due to the stress induced by the migration of Na_2O and K_2O inwards the crystal and the formation of the alkali metal carbonates during the reduction. Secondly, a remarkable growth of fibrous iron occurs inside the crack generated. It is considered that the growth is enhanced due to the lattice defects which come from the presence of alkali metal ions in hematite crystals. Thirdly, an intensified carbon deposition reaction occurs and it leads to the disintegration of the crystals.

Olivine pellets encompassed more cracks under potassium-containing conditions compared to the reference experiment carried out in $CO–CO_2–N_2$ atmosphere. Observed cracking behaviour led to volume increase of the pellets. Cracks inside a low-magnetite olivine pellet after reduction under potassium-containing conditions can be seen in **Fig. 16** in which LOM images captured from the core of a low-magnetite olivine pellet after (a) the "No additives" experiment, (b) the "Low-K" experiment and (c) the "High-K" experiment are presented. The cracking mechanism might be the stress caused by the migration of sodium and potassium inwards the pellet core as Nishikawa *et al.*[25] suggest. Potassium-containing phases were searched with FESEM but no especially K-rich phases were detected. Instead, potassium existed in small concentrations in the silicate phases as can be seen in **Fig. 17**. The figure shows an EDS mapping of elements from the periphery area of a low-magnetite olivine pellet reduced in the "High-K" experiment.

Secondary electron images by FESEM of medium-magnetite olivine pellet peripheries reduced to the reduction degree of 76–81% under certain reducing conditions are shown in **Fig. 18**. Each image has been taken at the same magnification in order to assure the comparability of the pellet structure. In image (a) there is no sulphur or potassium in reducing $CO–CO_2–N_2$ atmosphere ("No additives"), in image (b) sulphur is added to reducing $CO–CO_2–N_2$ atmosphere ("Medium-S") and in image (c) potassium is added to reducing $CO–CO_2–N_2$ atmosphere ("High-K"). The final reduction degree of the pellet is 76% in the "No additives" experiment, 80% in the "Medium-S" experiment and 81% in

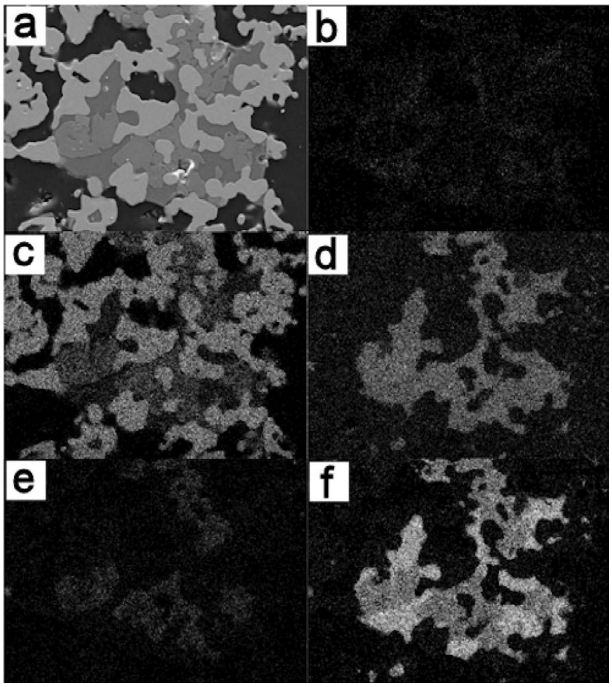

Fig. 17. FESEM-EDS mapping of elements in a low-magnetite olivine pellet in the "High-K" experiment. Figure (a) is the original backscattered electron image and the EDS mapping of elements is presented in (b) K, (c) Fe, (d) O, (e) Mg and (f) Si.

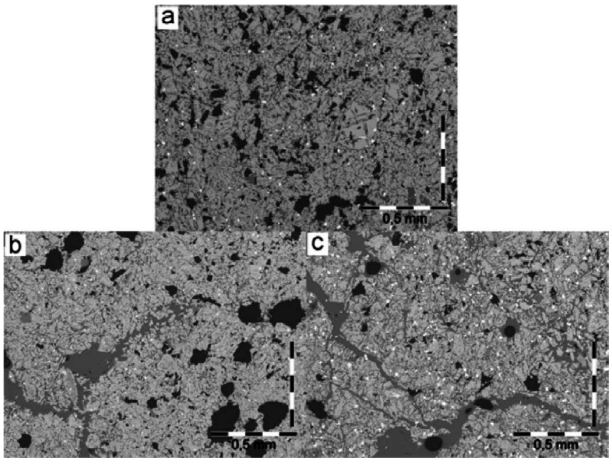

Fig. 16. LOM images from the core of a low-magnetite olivine pellet after (a) the "No additives" experiment, (b) the "Low-K" experiment and (c) the "High-K" experiment.

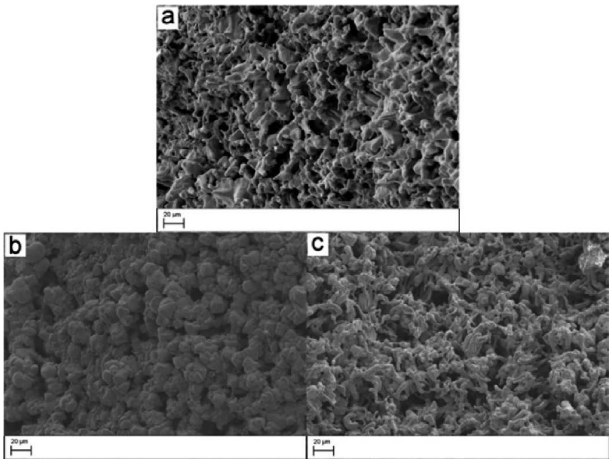

Fig. 18. Secondary electron images by FESEM of a medium-magnetite olivine pellet surface after dynamic reduction in the (a) "No additives" experiment, (b) "Medium-S" experiment and (c) "High-K" experiment.

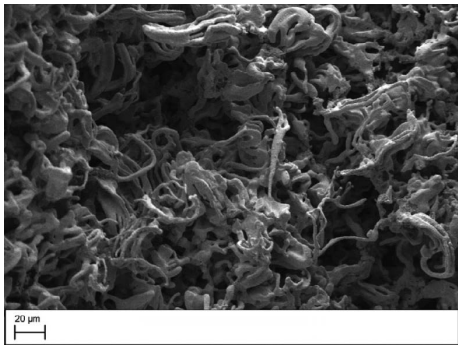

Fig. 19. Secondary electron image by FESEM of a high-magnetite olivine pellet surface in the cracking boundary. The pellet was reduced dynamically to a reduction degree of 76% in the "High-K" experiment.

the "High-K" experiment. In images a) and c) the pellet surface is covered by fibrous iron but in image b) representing sulphur addition, the surface structure is markedly denser which is consistent with the FeO–FeS liquid phase formation.

Surface structures resembling iron whiskers were detected in cracking boundaries of reduced pellets. **Figure 19** illustrates the cracking boundary of a high-magnetite olivine pellet photographed with FESEM after dynamic reduction in the "High-K" experiment to the final degree of reduction of 76%. It can be seen there the remarkable growth of fibrous iron that Nishikawa *et al.*[25] reported. The measured RSI value for the pellet is 22%.

5. Conclusions

In this study, the effect of gaseous sulphur and potassium on the dynamic reduction swelling behaviour of olivine and acid iron ore pellets under simulated blast furnace shaft conditions was investigated. The effect of gaseous sulphur was tested with three independent experiments containing a maximum of 0.01 vol-%, 0.10 vol-% and 1.0 vol-% sulphur in the reducing atmosphere. The effect of potassium on pellet swelling was tested with two experiments, the first one using a maximum of 0.015 vol-% potassium and the latter one a maximum of 0.03 vol-% in the reducing atmosphere during the experiment. The main implications drawn from the laboratory experiment results can be summarised as follows:

(1) No abnormal swelling (up to 20% in volume) occurred in $CO–CO_2–N_2$ atmosphere with sulphur or potassium in dynamic reduction when temperature was elevated at a moderate rate.

(2) Sulphur in the reducing atmosphere led to volume decrease of the pellets, being more marked in the acid pellets than in the olivine pellets. FeO–FeS liquid phases were formed under high sulphur partial pressure conditions at elevated temperatures preventing the reduction step of wüstite to metallic iron. Iron sulphide phases made the pellet periphery seem somewhat dense when imaging with FESEM.

(3) Large amounts of potassium, *e.g.* 0.03 vol-%, in the reducing atmosphere led to cracking based swelling in the olivine pellets, but not such a significant effect on the reduction swelling behaviour of the acid pellets could be seen. The crack formation was possibly due to the stress caused by the migration of potassium inwards the pellet core and the remarkable growth of fibrous iron in the cracking boundary.

(4) Olivine pellets encompassed more and larger cracks during dynamic reduction compared to acid pellets with different slag chemistry. Olivine pellets having a large magnetite nucleus were especially vulnerable to cracking based swelling due to the dualistic structure of a magnetite nucleus and a hematite shell. The swelling mechanism of olivine and acid pellets is more precisely discussed in the earlier paper by authors.[18]

Abbreviations

RSI	Reduction swelling index
BFS	Blast Furnace gas phase Simulator
LOM	Light optical microscope
FESEM	Field Emission Scanning Electron Microscope
EDS	Energy-Dispersive X-Ray Spectroscopy

Acknowledgements

Ruukki Metals Oy and the Finnish Funding Agency for Technology and Innovation (TEKES) are acknowledged for funding this work. Mr Tommi Kokkonen, Special Laboratory Technician with the University of Oulu, is acknowledged for his technical support. Parts of this paper are published in the 6th European Coke and Ironmaking Congress (ECIC) held in Düsseldorf, Germany in June 2011.

REFERENCES

1) W.-K. Lu and J. E. Holditch: Blast Furnace Conf.: HF80 Vol. 3, IRSID, Maizieres-les-Metz, (1980), III-3.
2) S. Hayashi and Y. Iguchi: *ISIJ Int.*, **29** (1989), 642.
3) H. Itaya, T. Fukutake, K. Okabe and T. Nagai: *Tetsu-To-Hagané*, **62** (1976), 472.
4) K. Lilius: *Scand. J. Metall.*, **9** (1980), 139.
5) A. K. Biswas: Principles of Blast Furnace Ironmaking: Theory and Practice, Cootha Publishing House, Brisbane, (1981), 528.
6) K. Orrebo: *Scand. J. Metall.*, **8** (1979), 67.
7) P. Mannila: Gas Phase Reactions in the Blast Furnace (in Finnish), Licenciate's thesis, University of Oulu, Finland, (1999), 89.
8) O. Mattila, J. Kurikkala, T. Paananen and T. Fabritius: METEC InSteelCon, 6th European Coke and Ironmaking Cong., Steel Institute VDEh, Düsseldorf, (2011).
9) S. Hayashi and Y. Iguchi: *ISIJ Int.*, **43** (2003), 1370.
10) S. Hayashi and Y. Iguchi: *Ironmaking Steelmaking*, **32** (2005), 353.
11) S. Hayashi, Y. Iguchi and J. Hirao: *Trans. Iron Steel Inst. Jpn.*, **26** (1986), 528.
12) P. L. Hooey, J. Sterneland and M. Hallin: 1st Int. Meeting on Ironmaking, Associacao Brasileira de Metalurgia e Materiais, Sao Paulo, (2001).
13) S. Hayashi: SCANMET III, 3rd Int. Conf. on Process Development in Iron and Steelmaking, Vol. 1, MEFOS, Luleå, (2008), 455.
14) S. Hayashi, Y. Iguchi and J. Hirao: *J. Jpn. Inst. Met.*, **48** (1984), 383.
15) S.-B. Lee and P. C.-H. Rhee: *Scand. J. Metall.*, **32** (2003), 203.
16) M. Bahgat, K. S. Abdel Halim, H. A. El-Kelesh and M. I. Nasr: *Ironmaking Steelmaking*, **36** (2009), 379.
17) W.-K. Lu: *Scand. J. Metall.*, **2** (1973), 65.
18) M. Iljana, O. Mattila, T. Alatarvas, V.-V. Visuri, J. Kurikkala, T. Paananen and T. Fabritius: *ISIJ Int.*, **52** (2012), 1257.
19) K. Blomster, P. Taskinen and J. Myyri: *Kemia-Kemi*, **2** (1975), 525.
20) J. L. Bailly, M. Picard, D. Sert, A. Succurro, M. Rougé and J. L. Reboul: A. Poos, Measuring Techniques in Blast Furnace Ironmaking and Their Benefits for Industrial Practice. ECSC workshop, Office for Officials Publications of the European Communities, Luxembourg, (1998), 139.
21) E. Beppler, M. Kannappel, W. Kowalski, K. Langner, K. Müllheims and H. Wachsmuth: A. Poos, Measuring Techniques in Blast Furnace Ironmaking and Their Benefits for Industrial Practice. ECSC workshop, Office for Officials Publications of the European Communities, Luxembourg, (1998), 111.
22) A. Kasai and Y. Matsui: *ISIJ Int.*, **44** (2004), 2073.
23) K.-H. Peters, E. Beppler, B. Gerstenberg and U. Janhsen: 53rd Ironmaking Conf. Proc., Iron and Steel Society, Warrendale, PA, (1994), 257.
24) Slag Atlas, ed. by Verein Deutscher Eisenhüttenleute, Verlag Stahleisen m.b.H., Düsseldorf, (1981), 282.
25) Y. Nishikawa, S. Sayama, Y. Ueda and Y. Suzuki: *Trans. Iron Steel Inst. Jpn.*, **23** (1983), 639.